

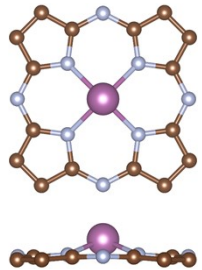
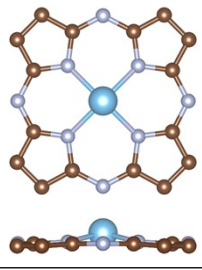
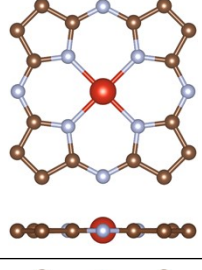
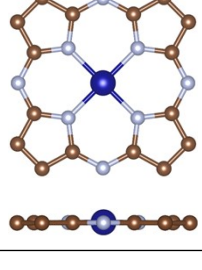
Supporting Information

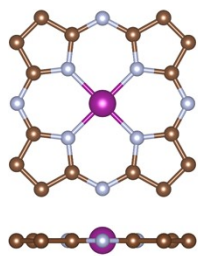
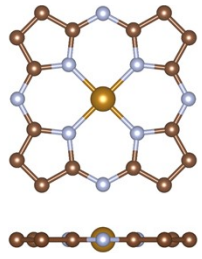
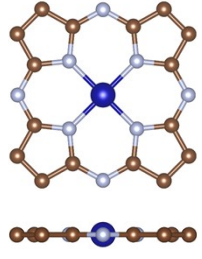
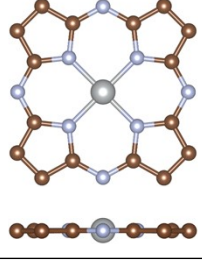
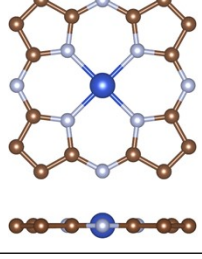
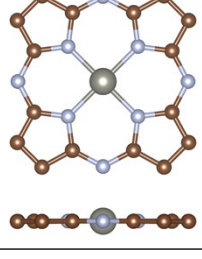
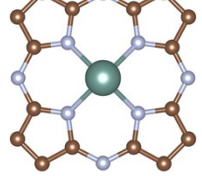
Two-Dimensional Metal-Organic TMTAP Monolayers as a Promising Class of Monoatomic Electrocatalysts for Oxygen Reduction, Oxygen Evolution, and Hydrogen Evolution Reactions

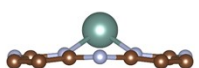
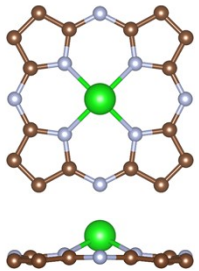
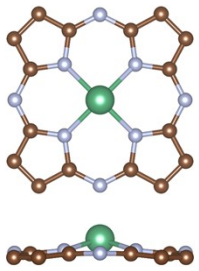
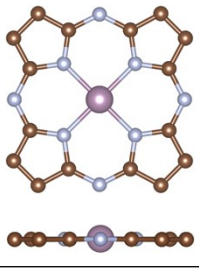
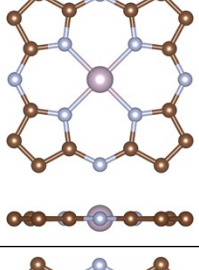
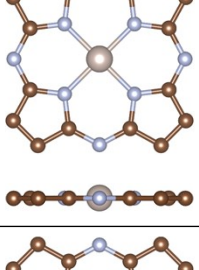
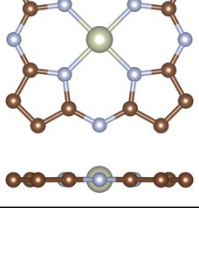
Debing Long, Xunyu Yang, Zihao Cheng, and Shan Peng*

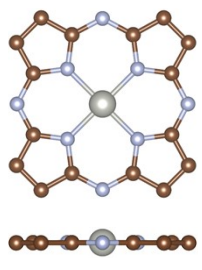
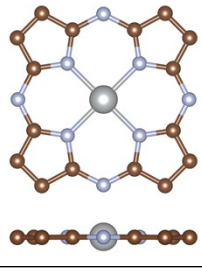
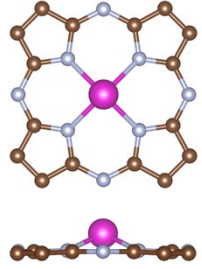
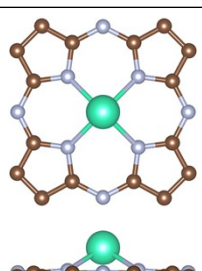
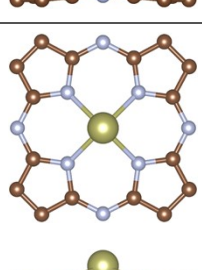
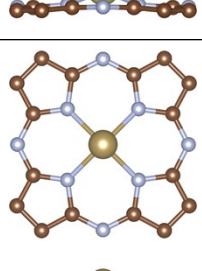
School of Physics and Electronic-Information Engineering, Hubei Engineering University, Xiaogan, 432000, P. R. China. (email: pengshan@hbeu.edu.cn)

Table S1. The relaxed geometric structure, lattice parameter (\AA), TM–N bond length (\AA), magnetic moment of TM atom (μ_B), and total magnetic moment (μ_B) for 30 TMTAP monolayers.

TMTA P	Geometric structure	Lattice parameter	TM–N bond length	Magnetic moment of TM	Total magnetic moment
Sc		8.34	2.11	0.36	0.59
Ti		8.34	2.04	1.39	1.63
V		8.33	1.99	2.51	2.68
Cr		8.32	1.99	3.49	3.84

Mn		8.29	1.96	2.73	3.03
Fe		8.27	1.93	1.72	2.00
Co		8.24	1.91	0.55	0.63
Ni		8.26	1.93	0.16	0.21
Cu		8.30	1.98	0.43	0.68
Zn		8.33	2.00	0	0
Y		8.34	2.25	0.19	0.57

					
Zr		8.34	2.16	0.81	1.58
Nb		8.35	2.08	1.62	2.54
Mo		8.38	2.05	2.94	3.64
Tc		8.35	2.02	2.20	2.74
Ru		8.31	1.98	0.32	0.34
Rh		8.30	1.98	0	0

Pd		8.31	1.99	0	0
Ag		8.38	2.06	0.42	0.89
Cd		8.37	2.16	0	0
Lu		8.34	2.21	0.15	0.60
Hf		8.35	2.11	0.67	1.11
Ta		8.35	2.07	1.77	2.23

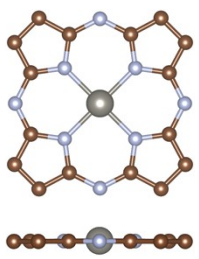
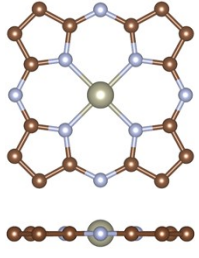
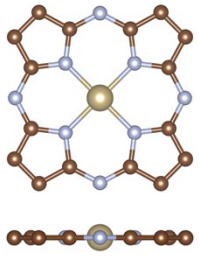
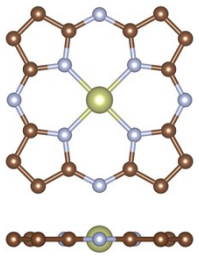
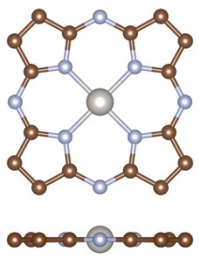
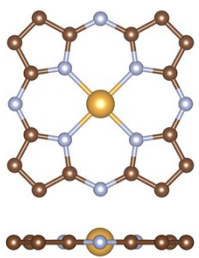
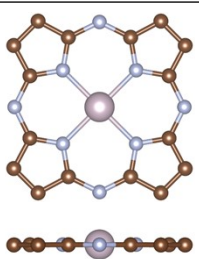
W		8.38	2.04	2.73	3.58
Re		8.36	2.02	1.94	2.64
Os		8.31	1.98	0	0
Ir		8.31	1.98	0	0
Pt		8.32	2.00	0	0
Au		8.37	2.05	0.31	0.64
Hg		8.45	2.13	0	0

Table S2. Calculated binding energies (E_b), cohesive energies ($E_c^{calc.}$), cluster energies ($E_{clus} = E_b + E_c$), and dissolution potentials of TM atoms (U_{diss}), number of transferred electrons during the dissolution (n). For comparison, the experimental cohesive energies ($E_c^{exp.}$) and standard dissolution potential (U_{diss}^o) of bulk metal are also listed.

TM	E_b (eV)	$E_c^{exp.}$ (eV)	$E_c^{calc.}$ (eV)	E_{clus} (eV)	n	U_{diss}^o (V)	U_{diss} (V)
Sc	-8.76	3.90	4.36	-4.40	3	-2.08	-0.61
Ti	-9.13	4.90	5.5	-3.63	2	-1.63	0.19
V	-8.50	5.30	5.4	-3.10	2	-1.18	0.37
Cr	-7.34	4.10	4.05	-3.29	2	-0.91	0.73
Mn	-6.82	2.90	3.29	-3.53	2	-1.19	0.57
Fe	-7.52	4.30	4.63	-2.89	2	-0.45	0.99
Co	-8.12	4.40	5.09	-3.03	2	-0.28	1.23
Ni	-7.44	4.40	4.74	-2.70	2	-0.26	1.09
Cu	-5.38	3.50	3.49	-1.89	2	0.34	1.29
Zn	-3.98	1.40	1.17	-2.81	2	-0.76	0.65
Y	-8.53	4.40	4.28	-4.25	3	-2.37	-0.95
Zr	-9.31	6.30	6.27	-3.04	4	-1.45	-0.69
Nb	-8.61	7.60	7.02	-1.59	3	-1.10	-0.57
Mo	-7.30	6.80	6.36	-0.94	3	-0.20	0.11
Tc	-8.06	6.90	7.07	-0.99	2	0.30	0.79
Ru	-8.47	6.70	7.03	-1.44	2	0.46	1.18
Rh	-8.33	5.80	5.98	-2.35	2	0.60	1.77
Pd	-6.12	3.90	3.74	-2.38	2	0.95	2.14
Ag	-3.08	3.00	2.82	-0.26	1	0.80	1.06
Cd	-2.21	1.20	0.94	-1.27	2	-0.40	0.23
Lu	-8.38	4.43	4.32	-4.06	3	-2.28	-0.93
Hf	-9.75	6.40	6.79	-2.96	4	-1.55	-0.81
Ta	-9.68	8.10	8.47	-1.21	3	-0.60	-0.20
W	-8.61	8.90	8.49	-0.12	3	0.10	0.14

Re	-7.76	8.00	7.82	0.06	3	0.30	0.28
Os	-9.06	8.20	8.43	-0.63	8	0.84	0.92
Ir	-9.42	6.90	7.56	-1.86	3	1.16	1.78
Pt	-8.20	5.80	5.72	-2.48	2	1.18	2.42
Au	-3.44	3.80	3.46	0.02	3	1.50	1.49
Hg	-0.26	0.70	0.58	0.32	2	0.85	0.69

^{a)}Experimental cohesive energy values are taken from ref. 1 [1].

^{b)}Standard dissolution potential values are taken from ref. 2 [2].

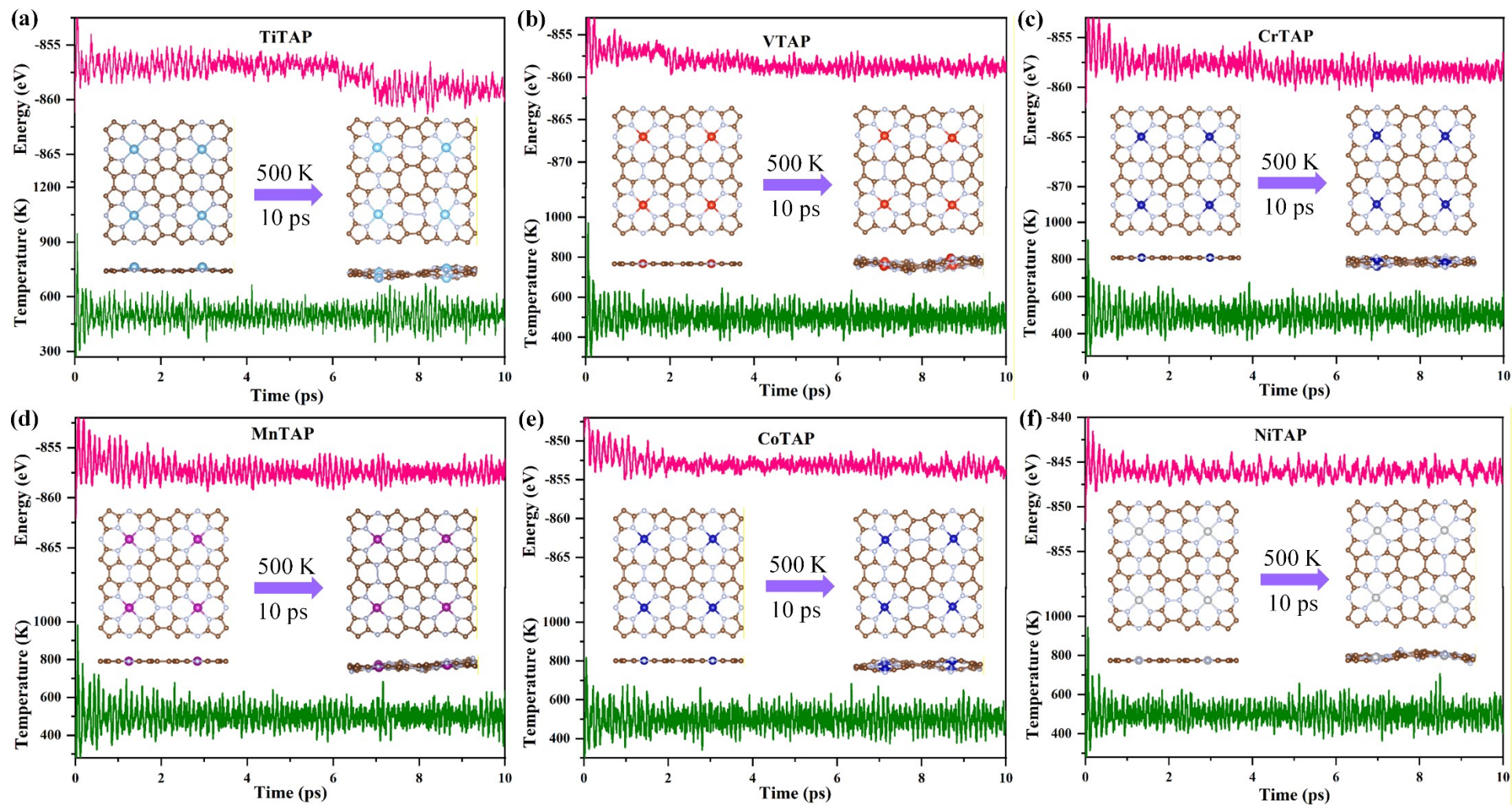


Figure S1. Evolution of the temperatures and total energies of AIMD simulations for (a) TiTAP, (b) VTAP, (c) CrTAP, (d) MnTAP, (e) CoTAP, and (f) NiTAP at 500 K for 10 ps with a time step of 2 fs. The illustrations are snapshots of the initial and final frame during AIMD simulations.

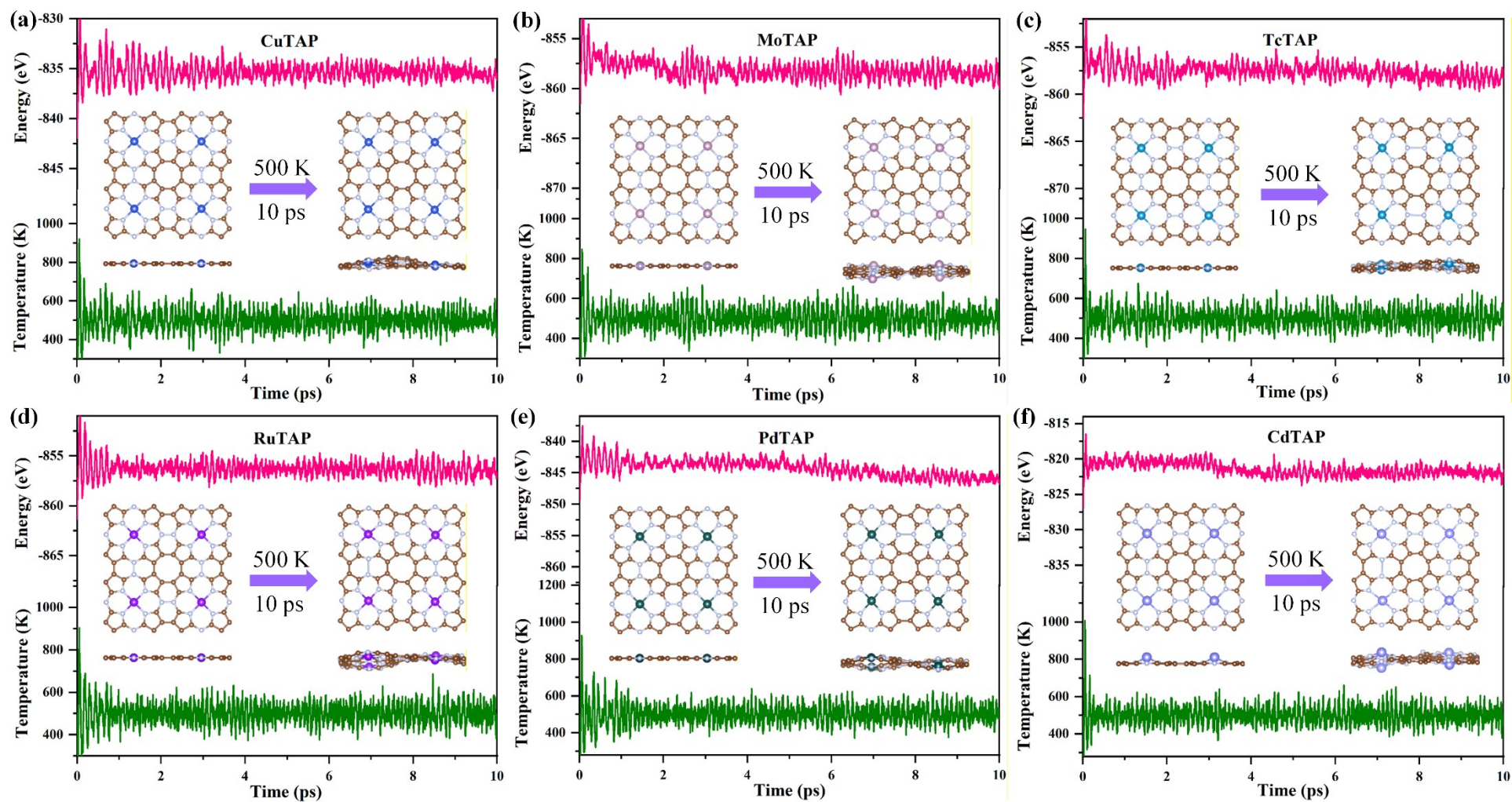


Figure S2. Evolution of the temperatures and total energies of AIMD simulations for (a) CuTAP, (b) MoTAP, (c) TcTAP, (d) RuTAP, (e) PdTAP, and (f) CdTAP at 500 K for 10 ps with a time step of 2 fs. The illustrations are snapshots of the initial and final frame during AIMD simulations.

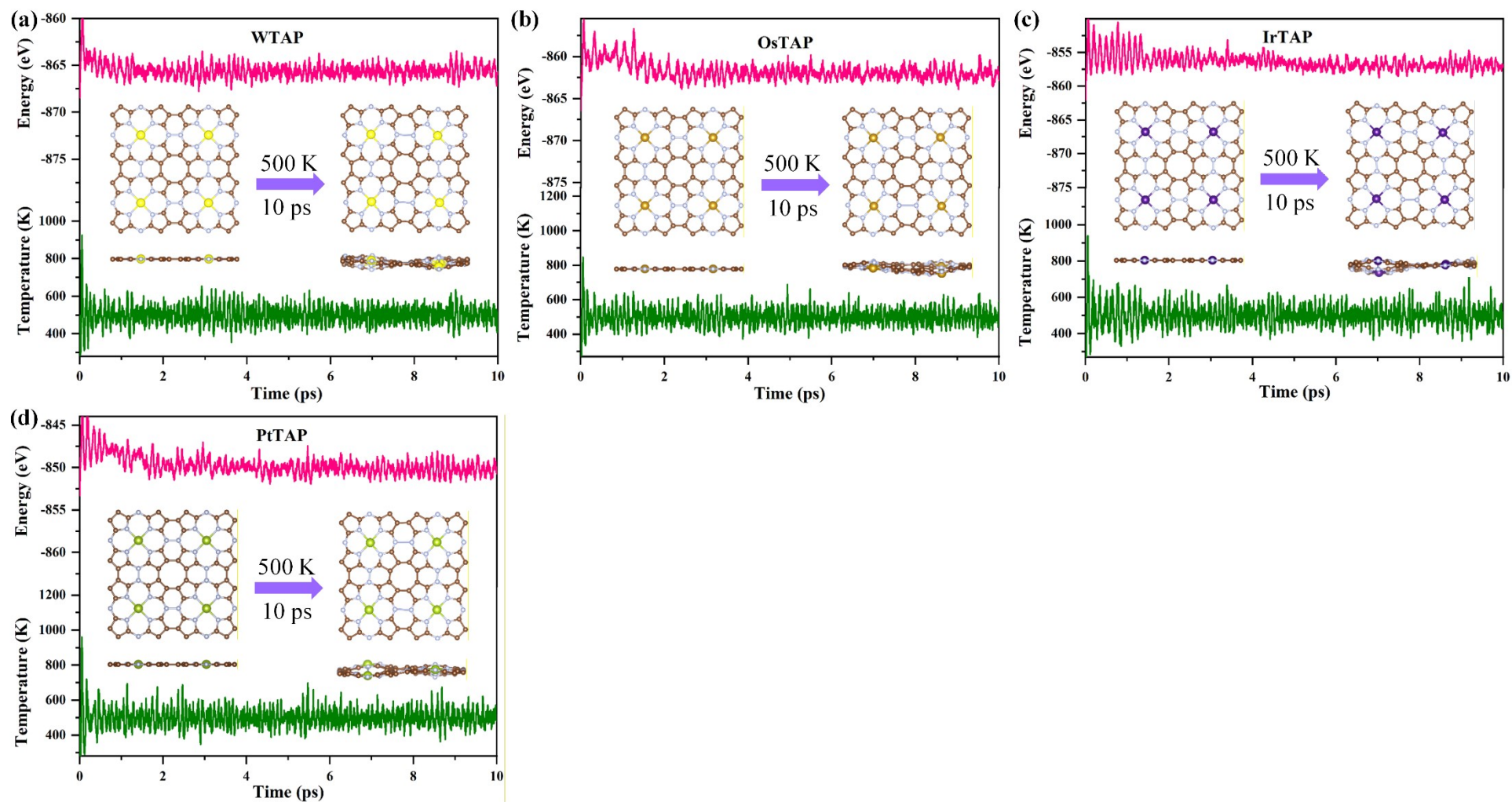


Figure S3. Evolution of the temperatures and total energies of AIMD simulations for (a) WTAP, (b) ReTAP, (c) OsTAP, (d) IrTAP, and (e) PtTAP at 500 K for 10 ps with a time step of 2 fs. The illustrations are snapshots of the initial and final frame during AIMD simulations.

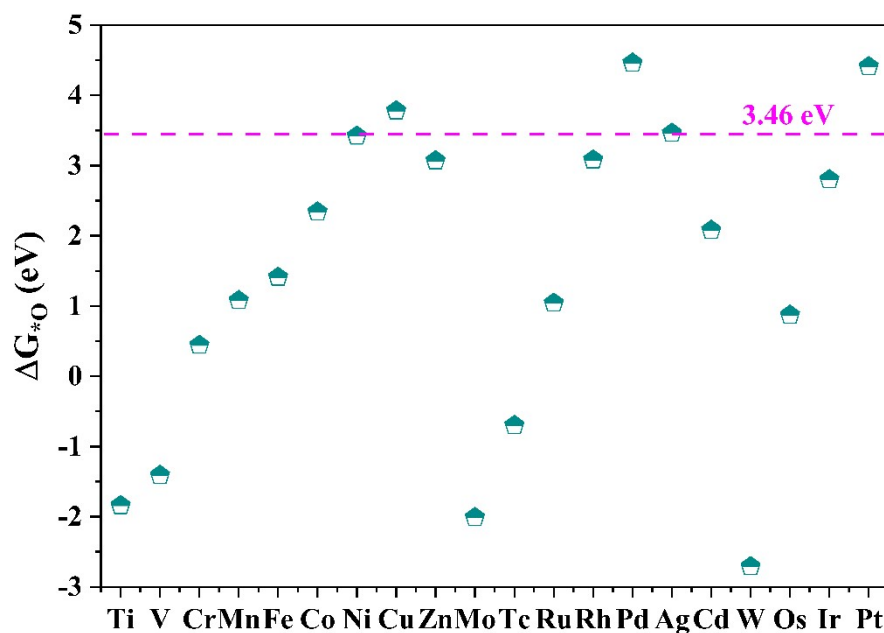


Figure S4. Calculated ΔG_{*O} values of the 20 stable SACs. The horizontal dotted line is $\Delta G_{*O} = \Delta G_{H_2O_2} - \Delta G_{H_2O} = 3.46$ eV.

Table S3. Summary Table of Benchmarking SACs.

Catalyst	Support	Reaction	Overpotential (V)	Literature
MnPor	metalloporphyrinoid (MPor)	ORR	0.56	<i>Rare Met.</i> 2025, 44, 3920–3933
Fe-Pc	Phthalocyanine (Pc)	ORR	0.45	<i>Int. J. Hydrogen Energy</i> 2024, 88, 850–857
Mn ₃ (HHTP) ₂	2,3,6,7,10,11-hexahydroxytriphenylene (HHTP)	ORR/OER	0.44/0.53	<i>J. Phys. Chem. C</i> 2025, 129 (31), 14002–14010
Rh ₃ (HADQ) ₂	2,3,6,7,10,11-hexamine (C ₁₂ H ₁₂ N ₁₂) pyrazine quinoxaline (HADQ)	ORR/OER	0.31/0.31	<i>Langmuir</i> 2025, 41 (1), 745–754
Cu@g-C ₄ N ₃	g-C ₄ N ₃	ORR	0.70	<i>ACS Appl. Mater. Interfaces</i> 2024, 16 (14), 17617–17625
Co@C ₃ N ₂	C ₃ N ₂	HER	0.12	<i>New J. Chem.</i> 2025, 49, 1672–1685
Mn ₁₂ C ₁₂	carbon layer	HER	0.09	<i>Int. J. Hydrogen Energy</i> 2025, 144, 1043–1050
ZnTAP	TAP	ORR	0.43	<i>This work</i>
RhTAP	TAP	OER	0.58	<i>This work</i>
CdTAP	TAP	HER	0.08	<i>This work</i>

Table S4. The adsorption free energies of *OOH (ΔG_{*OOH}), *O (ΔG_{*O}), and *OH (ΔG_{*OH}) on TMTAP.

TMTAP	ΔG_{*OOH} (eV)	ΔG_{*O} (eV)	ΔG_{*OH} (eV)
Ti	1.91	-1.84	-1.66
V	1.22	-1.41	-0.54
Cr	3.70	0.44	0.48
Mn	3.85	1.08	0.66
Fe	3.80	1.41	0.76
Co	4.40	2.34	1.50
Ni	4.94	3.42	1.95
Cu	4.85	3.78	2.00
Zn	4.02	3.07	0.80
Mo	-0.34	-2.01	-0.46
Tc	1.78	-0.70	-0.02
Ru	3.54	1.04	0.79
Rh	4.89	3.08	1.78
Pd	5.13	4.46	2.46
Ag	4.55	3.46	7.42
Cd	2.91	2.08	-0.36
W	-1.58	-2.71	-0.98
Re	0.84	-1.45	-0.30
Os	3.33	0.87	0.95
Ir	4.88	2.80	1.80
Pt	5.13	4.41	2.46

Table S5. The bond length of adsorbed O₂ molecule (Å), magnetic moment of TM atom (μ_B) before and after O₂ adsorption for Fe-, Zn-, Rh-, and AgTAP catalysts.

TMTAP	Bond length of adsorbed O ₂ molecule	Magnetic moment of TM atom before O ₂ adsorption	Magnetic moment of TM atom after O ₂ adsorption
Fe	1.29	1.72	1.87
Zn	1.30	0	0.01
Rh	1.27	0	0.32
Ag	1.27	0.42	0.12

Table S6. Calculated Bader charges on TM and O atoms, magnetic moment of O atom (μ_B) after O₂ adsorption for Fe-, Zn-, Rh-, Ag-, Ti-, Mo-, and W-TAP catalysts.

TMTAP	TM	O	Magnetic moment of O
Fe	-1.13 e	+0.22 e	0.63
Zn	-1.26 e	+0.25 e	0.56
Rh	-0.77 e	+0.15 e	0.70
Ag	-0.69 e	+0.13 e	0.68
Ti	-1.65 e	+0.48 e	0.01
Mo	-1.54 e	+0.47 e	0
W	-1.76 e	+0.49 e	0.01

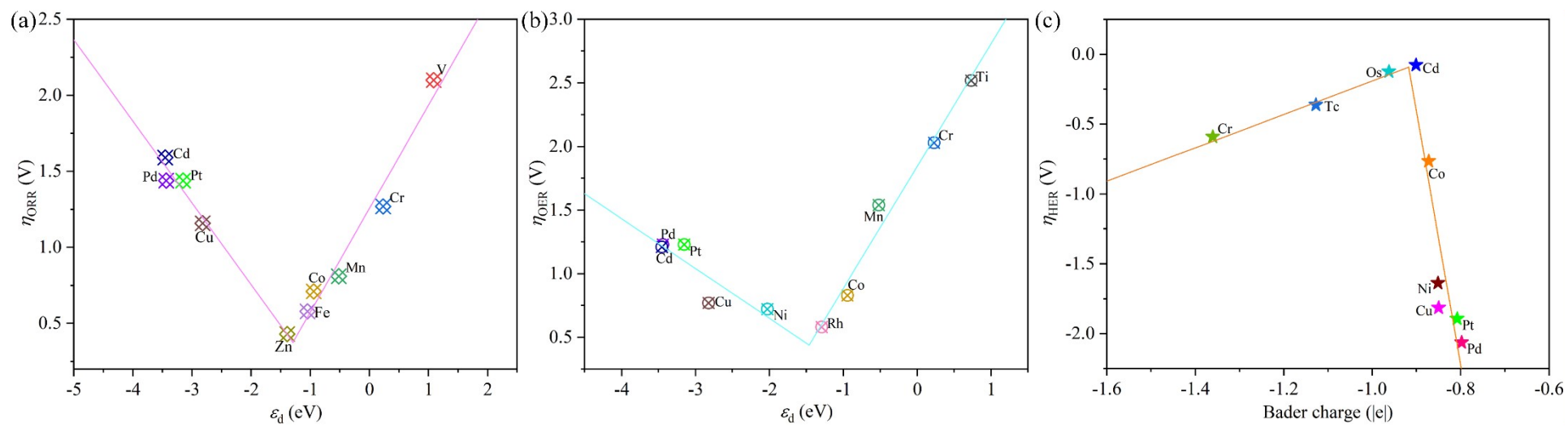


Figure S5. Volcano plot of the η_{ORR} as a function of the d-band center (ϵ_d). (b) Volcano plot of the η_{OER} as a function of the d-band center (ϵ_d). (c) Volcano plot of the η_{HER} as a function of the Bader charge.

References

- [1] Kittel, C., *Introduction to solid state physics*. Wiley, Hoboken, **2005**.
- [2] Landolt–Bornstein, N. D., *Functional Relationships in Science and Technology*. Springer, Berlin, **1982**.